Khzouz, M. et al. (2013). Characterization and activity test of commercial Ni/Al_20_3, Cu/ZnO/Al_20_3 and prepared NieCu/Al_20_3 catalysts for the hydrogen production from methane and methanol fuels.
International Journal of Hydrogen Energy, 38: 1664 – 1675.
http://dx.doi.org/10.1016/j.ijhydene.2012.07.026

Characterization and activity test of commercial Ni/Al2O3, Cu/ZnO/Al2O3 and prepared NieCu/Al2O3 catalysts for hydrogen production from methane and methanol fuels

Martin Khzouz, Joe Wood, Bruno Pollet and Waldemar Bujalski

Abstract

In this study, methane and methanol steam reforming reactions over commercial Ni/Al_2O_3, commercial Cu/ZnO/Al_2O_3 and prepared NieCu/Al_2O_3 catalysts were investigated. Methane and methanol steam reforming reactions catalysts were characterized using various techniques. The results of characterization showed that Cu particles increase the active particle size of Ni (19.3 nm) in NieCu/Al_2O_3 catalyst with respect to the commercial Ni/ Al_2O_3 (17.9). On the other hand, Ni improves Cu dispersion in the same catalyst (1.74%) in comparison with commercial Cu/ZnO/Al_2O_3 (0.21%). A comprehensive comparison between these two fuels is established in terms of reaction conditions, fuel conversion, H_2 selectivity, CO_2 and CO selectivity. The prepared catalyst showed low selectivity for CO in both fuels and it was more selective to H_2, with H_2 selectivities of 99% in methane and 89% in methanol reforming reactions. A significant objective is to develop catalysts which can operate at lower temperatures and resist deactivation. Methanol steam reforming is carried out at a much lower temperature than methane steam reforming in prepared and commercial catalyst (275-325 ^{0} C). However, methane steam reforming can be carried out at a relatively low temperature on NieCu catalyst (600-650 ^{0} C) and at higher temperature in commercial methane reforming catalyst (700-800 ^{0} C). Commercial Ni/Al_2O_3 catalyst resulted in high coke formation (28.3% loss in mass) compared to prepared NieCu/Al_2O_3 (8.9%) and commercial Cu/ZnO/Al_2O_3 catalysts (3.5%).

1. Introduction

About 700 billion Nm^3 of hydrogen is produced around the world and most of this hydrogen is produced on-site for industrial use [1]. The large and small scale production of hydrogen is likely to contribute to the energy market in the short to medium term in Europe [2]. However, the hydrogen produced at both scales requires an infrastructure network for storage, transmission and distribution, which is largely yet to be developed.

The hydrogen produced on-board in vehicles from its energy carriers can solve the technical problem of storing and distribution of hydrogen [3]. This can be achieved by using fuel processing technology. Hydrocarbons or alcohols are converted to pure hydrogen using a fuel reformer (fuel processor). Utilizing the hydrogen produced in proton exchange membrane fuel cell (PEMFC) to generate electricity could solve the future energy problems in transportation and domestic applications [4].

Steam reforming (equation (1)) is widely used in industry to generate syngas (H_2

$$C_nH_mO_z + (n-z)H_2O \rightarrow nCO + \left(n - z + \frac{m}{2}\right)H_2 \qquad (1)$$

Steam reforming is an endothermic reaction between the reactants (hydrocarbons and steam) which will need a significant amount of energy to activate the reaction. The reaction in the fuel reformer depends on several factors; the temperature required for fuel reforming, the level of by products that the connected system can tolerate, the daily cycle of the reformer and the fuel used to produce hydrogen [7]. The choice of a suitable fuel reformer and fuel is the key aspects to the successful implementation of hydrogen fuel cell system [8]. A reformer integrated to a fuel cell is an attractive fuel source for the low temperature fuel cell such as PEMFC [9], which requires a high purity of hydrogen [10]. On the other hand, internal reforming in the fuel cell stack itself, could only be used with high temperature fuel cells such as solid oxide fuel cell (SOFC) and after taking into consideration a large amount of CO in the reformate stream [11,12]. Table 1 shows the fuel that can be used for transportation and residential use applications [13].

Hydrogen can be extracted via methanol steam reforming. The endothermic methanol steam reforming reaction (equation (2)) is the most frequently used method and it is possible to yield a gas product containing up to 75% hydrogen [14]. Although methanol has several disadvantages especially with regards to its distribution network [15], it is still a strong candidate fuel for fuel cell vehicles as the overall processing system would be simpler than other hydrocarbon fuels [16,17]. In addition, methanol could be sold in single-use containers for use in portable fuel cell units for low power applications [15].

Table 1 – Characteristics of steam reforming process for producing hydrogen via intermediate fuels [13].

Steam reforming of	CO in product (mol%) initial reaction	Temperature range of initial reaction (°C)	Total theoretical input energy to process (kJ/kg of usable H_2)
Methane	11.2	727–827	0.141
Methanol	0.8	227–287	0.145
Ethanol	10–14	~527–727	0.144
Gasoline, diesel fuel and aviation jet fuel	20	727–877	0.148

Methanol reforming process is carried out at a temperature range of 200-300 based catalysts which usually consist of $Cu/ZnO/Al_2O_3$ [6]. The steam reforming of methanol (equation (2)) would ideally produce hydrogen and carbon dioxide. However, this is not the case in the actual process, the reformate gases usually contain CO, CO_2, H_2, H_2O, CH_3OH and other intermediate species produced via methanol decomposition reaction (equation (3)) and water gas shift reaction (equation (4)) [18-20].

$$CH_3OH + H_2O \rightarrow CO_2 + 3H_2,\ \Delta H^0_{298} = +49.5\ kJ/mol \quad (2)$$

$$CH_3OH \rightarrow CO + 2H_2,\ \Delta H^0_{298} = +90.2\ kJ/mol \quad (3)$$

$$CO + H_2O \rightarrow CO_2 + H_2,\ \Delta H^0_{298} = -41\ kJ/mol \quad (4)$$

Steam reforming of methane (equation (5)) produces hydrogen and carbon monoxide in a ratio of three to one. This main reaction is followed by a water gas shift process where carbon monoxide is converted into hydrogen and carbon dioxide as shown in (equation (4)) [21]. The steam reforming of methane can be represented as the sum of steam reforming of methane and the water gas shift reaction as shown in (equation (6)). The reaction is operated at high temperature (800 ^{0} C) over nickelealumina based catalysts since high conversion of methane is achieved at this temperature [22]. A typical composition of reformed gas contains H_2, CO_2, unconverted methane and CO [23].

$$CH_4 + H_2O \rightarrow CO + 3H_2, \Delta H^0_{298} = +206\ kJ/mol \quad (5)$$

$$CH_4 + 2H_2O \rightarrow CO_2 + 4H_2, \Delta H^0_{298} = +165\ kJ/mol \quad (6)$$

Catalyst development is essential for designing an efficient, compact, fast start up and a low cost reformer [7]. Heterogeneous catalysts are majorly employed in steam reforming reactions so the reactants can readily pass through a solid catalyst bed [24]. These catalysts are categorized into three types: oxide catalysts, noble metal catalysts and base metal catalysts as illustrated in Table 2 [5]. A copper based catalyst is active at low temperature but its selectivity towards H_2 is low. In comparison with a copper based catalyst, a nickel based catalyst is highly selective towards H_2 at high temperature. However, it suffers from high coke formation and a severe deactivation.

In this work both methane and methanol steam reforming reactions on commercial Ni/Al_2O_3 and commercial $Cu/ZnO/Al_2O_3$ respectively have been studied. $NieCu/Al_2O_3$ catalyst was prepared and tested for both reactions, with the aim to increase the catalytic activity, lower the amount of carbon monoxide produced and develop a catalyst with a higher carbon tolerance. NieCu catalysts have been previously studied for ethanol steam reforming [25e28], methane decomposition reaction [29e31], methane partial oxidation [32] and methanol steam reforming reactions [33]. It was reported in those studies that copper existence suppresses carbon formation. However, methanol and methane steam reforming reactions were not explored widely for such type of catalyst as well as compared to their commercial counterpart. Therefore, in the present study, a bimetallic catalyst which could show a high selectivity towards hydrogen and resist carbon deactivation in methane and methanol reforming compared with commercially available catalysts is investigated. The chemical and physical properties and catalytic performance are explored in this study. Catalyst characterization and activity tests are presented and comprehensive comparison for hydrogen generation via methane and methanol fuels are discussed.

Table 2 – Summary of the advantages and disadvantages of reforming catalysts from the literature [5].

Category	Example	Properties
Oxide catalysts	MgO, Al_2O_3, V_2O_5, ZnO, TiO_2, La_2O_3, CeO_2, La_2O_3–Al_2O_3, CeO_2–Al_2O_3, MgO–Al_2O_3	Normally good activity but low selectivity.
Noble metal catalysts	Rh, Ru, Pt and Pd	Active, high selectivity but the cost is high.
Base metal catalysts	Co-based (Co/ZnO), Cu-based and Ni-based (Ni/Al_2O_3)	Co-based: good catalytic performance, but rapidly deactivate. Cu-based: good activity at low reaction temperature, while H_2 selectivity is poor. Ni-based: high conversion and the H_2 selectivity, but may occur coke deposition and a severe deactivation.

2. Experimental

2.1 Catalyst

Two commercial reforming catalysts were selected to provide a basis for comparison with custom made catalysts. Copper based methanol reforming catalyst, HiFUEL R120 (Alfa Aesar) and nickel based steam reforming catalyst, HiFUEL R110 (Alfa Aesar) were characterised and tested for both methanol and methane steam reforming respectively. 5%Nie5%Cu/Al_2O_3 catalysts were prepared using an impregnation method and the metal loadings in prepared catalyst were tested using X-ray fluorescence (XRF) Bruker S8 Tiger spectrometer type. Briefly, the metal solution (0.8 M) of nickel nitrate ($Ni(NO_3)_2.6H_2O$) and copper nitrate ($Cu(NO_3)_2.3H_2O$) provided by Fisher Scientific were prepared using 13.8 ml ethanol (Fisher scientific) with 99.8% purity. Six grams of Al_2O_3 (Johnson Matthey) trilobe-shaped catalyst supports were added to the solution and it was mixed for 2 h using a Bandelin Sonorex bath at 27 ^{0} C. The catalyst was dried in a static oven overnight at 100 ^{0} C, then the catalyst was heated for calcination to 500 ^{0} C at a rate of 5 ^{0} C/min, held at that temperature for 5 h, then finally cooled at rate of 5 ^{0}C/min to ambient temperature. The prepared catalyst was tested for both methanol and methane steam reforming reactions.

2.2. Characterization

The catalysts were characterized using scanning electron microscope (SEM), Brunauer Emmett Teller (BET) surface area test, CO chemisorption, X-ray diffraction (XRD), infrared (IR), and temperature programmed reduction (TPR) analyses.

SEM (Philips XL-30) of the catalyst was performed after coating with gold. BET surface area measurements [34] were performed using a Micrometrics ASAP 2010 analyzer. Samples were measured using N_2 physisorption isotherms at -196 ^{0}C. CO chemisorption tests were performed on a Micrometrics AutoChem 2920 Analyzer. Briefly, one gram of crushed catalyst was reduced using 10% H_2 in Argon at a flow rate 10 ml/min at 450 ^{0}C for 2 h. Helium gas was then introduced at a flow rate of 10 ml/min and the sample was cooled to ambient temperature. Finally, CO adsorption was investigated at a temperature of 30 ^{0}C at a flow rate of 20 ml/min and helium as a carrier gas at a flow rate of 50 ml/min. Pulses of volume of 0.5389 ml (loop volume) were applied twenty times and any remaining CO which was not adsorbed on the catalyst was detected by a thermal conductivity detector (TCD) in the gas stream flowing from the tube outlet.

XRD was performed on a Bruker D8 Advance diffractometer using Cu Ka radiation (l = 0.154 nm). The data was recorded at room temperature in the two theta range from 5^0 to 90^0. Infrared spectra for catalysts were recorded using a Bruker Tensor 37. The crushed catalyst was sieved with KBr at a particle size less than 75 mm and 64 scans of absorbed spectra were monitored in the range 400-4000cm^{-1}.

TPR experiments were investigated on one gram of sample using a Micrometrics AutoChem 2920 Analyzer. The sample was reduced at 500 ^{0}C for 1 h using 10% H_2 in Argon then the sample was cooled to ambient temperature. Finally, the temperature was increased to 900 ^{0}C at 10 ^{0}C/min and hydrogen uptake was recorded using a TCD.

2.3. Activity test

The multi fuel reformer experimental test rig was used to test the catalyst activity and selectivity for H_2, CO_2 and CO production. It consists of three modules; feeding module, reactor module and gas analysis module as shown in Fig. 1.

In methanol steam reforming, distilled water is mixed with pure methanol (99.99%) at a ratio of 1.7. The premix of methanol and water was injected to the reactor feed line using a Cole-Palmer EW-74930-05 series one pump to the vaporizer (110 ^{0}C) at a constant flow rate of 0.06 ml/min. On the other hand, methane steam reforming was carried out by injecting pure methane (99.99%) into the reactor feed line at a flow rate of 25 ml/min and controlled by a Brooks mass flow controller. The steam

generated as the water flowed through the trace heated section at temperature (110 ^{0}C) is mixed with methane at ratio 3:1.

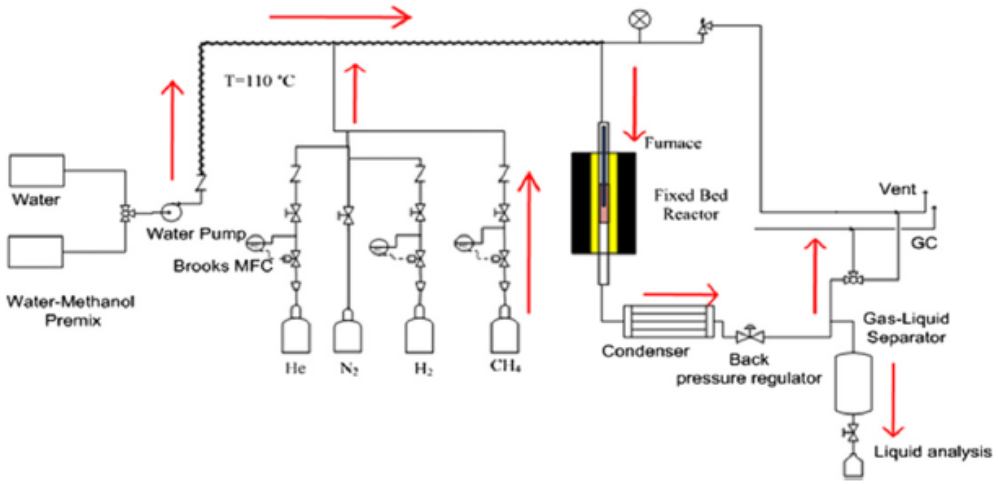

Fig. 1 – Multi fuel reformer experimental test rig.

The reactor was constructed of stainless steel tube (316 l) with inside diameter 15.6 mm and 395 mm length; the wall thickness of the pipe is 3.45 mm. The catalyst was packed in the reactor to a bed height of 26 mm for both reactions using a catalyst weight of 3 g. The temperature inside the furnace was measured using K type thermocouple which is fixed at the centre of the bed and the temperature of the furnace was controlled using a PID controller.

A gas chromatograph (Agilent 7890A) was used to detect hydrocarbons compounds, CO, CO_2 and H_2. The gas chromatograph was configured as a multi column instrument refinery gas analyzer. TCD2 back signal was used to detect methane, CO_2 and CO. The other auxiliary TCD was used to detect hydrogen only. The flame ionization detector (FID) was used to measure multi hydrocarbon bonded compounds and any organic by products produced. The un-reacted water and methanol mixture were separated from the gaseous stream using a condenser. The condensation process was facilitated by ice cubes in a bath surrounding the pipe at a temperature of -2 ^{0}C. The gaseliquid separator separates a gas stream from the un-reacted methanol mixture and water. The unconverted liquid reactants were analyzed using a Thermo Trace GC Ultra, which has a Thermo TR-5ms SQC column that detects water and methanol concentrations. A sample of 0.1 ml was injected. The oven temperature of the GC was ramped from 35 ^{0}C to 100 ^{0}C at a rate of 5 ^{0}C/min and it was held at that temperature for 2 min.

The catalyst was reduced in situ using pure hydrogen at a flow rate of 10 ml/min. Both commercial Ni/Al_2O_3 and prepared $NieCu/Al_2O_3$ were reduced at a temperature of 550 ^{0}C and commercial $Cu/ZnO/Al_2O_3$ at 250 ^{0}C. The temperature

was raised at a rate of 5 ^{o}C/min under an atmosphere of pure hydrogen at a flow rate of 10 ml/min. When the temperature of reduction was reached, hydrogen was injected for 30 min in the reduction procedure before switching to pure N_2 for purging purposes. Methanol steam reforming was carried out at temperatures (250, 275, 300, 325 ^{o}C) and methane steam reforming at temperatures (500, 550, 600, 650, 700 ^{o}C) in order to find the optimum operating conditions. The warm up period for reaction was 1 h. After that, reformates were sampled every 15 min for 3 h of operation.

3. Results and discussion

3.1 SEM test

Fig. 2 shows SEM images for tested catalysts at 90 mm scale. The images show the textural distribution of metals on support on micro scale. It is clear from Fig. 2(a)-(c) that each catalyst has its own metal clusters on the support with various sizes [35].

3.2. BET and CO chemisorptions tests

Table 3 summarizes the physical characteristics of catalysts. The prepared NieCu/Al_2O_3 catalysts showed high surface areas and pore volumes compared to commercial catalysts. Low pore volume in commercial Ni/Al_2O_3 catalysts can be interpreted as being due to high metal loading through which Ni particles might block pores of Al_2O_3 during metal deposition [32,33]. The CO chemisorption experiment revealed that NieCu/Al_2O_3 catalyst has a higher metallic surface area and metal dispersion than commercial Cu/ZnO/Al_2O_3 and Ni/Al_2O_3 catalysts. De Rogatis et al. [32] had prepared NieCu/Al_2O_3 catalyst which showed a BET surface area of 82 m^2/g. On the other hand, the commercial catalyst of Ni/Al_2O_3 studied by Hou and Hughes [36] resulted in a BET surface area of 14.30 m^2/g, which is slightly higher than commercial catalyst tested in the present study (12 m^2/g). The commercial Cu/Zno/ Al_2O_3 catalyst studied by Jones and Hagelin-Weaver [37] showed a BET surface area of 68 m^2/g [37]. Ginés et al. [38] had studied the metallic copper dispersion and it was observed that the copper dispersion varied between a minimum value of 0.5% and a maximum value of 5%. This was interpreted to the amount of hydrotalcite contained in the hydroxycarbonate precursor, the higher the hydrotalcite content leads to the higher the copper metal dispersion in the resulting catalyst.

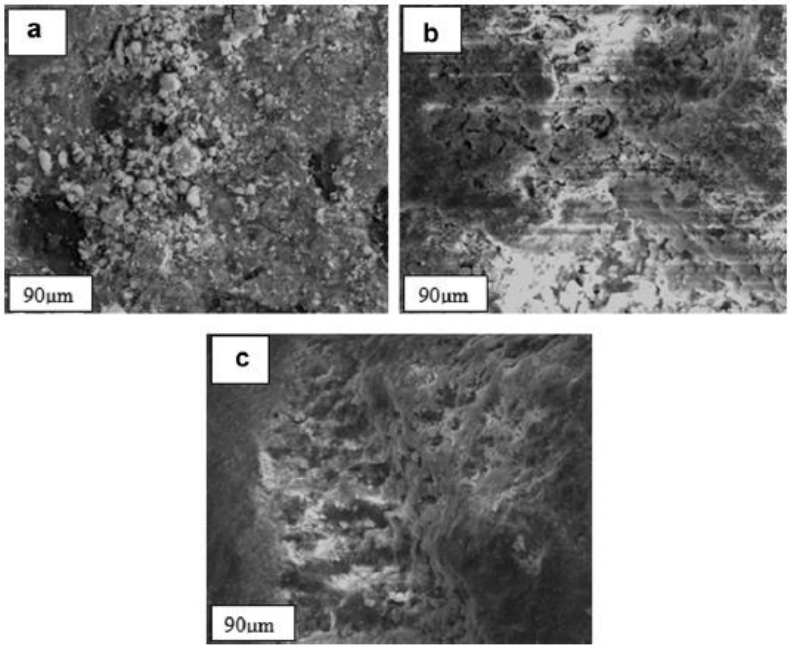

Fig. 2 – SEM of (a) $Cu/ZnO/Al_2O_3$, (b) Ni/Al_2O_3, (c) $Ni–Cu/Al_2O_3$.

In this study, a lower value of dispersion (0.21%) was observed due two main reasons, namely; the large particle size of copper and the conventional preparation method (co-precipitation) used [39e42]. The value of dispersion reported here (1.29%) for commercial Ni/Al_2O_3 catalyst is similar to one reported by Oliveira et al. [43] (1.42%) and by Seo et al. [44] (1.5%). Prepared $NieCu/Al_2O_3$ catalyst showed a metal dispersion slightly higher than commercial Ni catalyst. However, prepared catalyst in this study had low metallic dispersion (1.74%) compared to the prepared catalyst (4.1%) studied by De Rogatis et al. [33]. This can be related to the large particle size of present catalyst and several treatment conditions during impregnation method such; calicination temperature and type of the support used [38].

3.3. XRD test

XRD test from 5^0 to 90^0 in Fig. 3 shows the characteristics peaks of metal oxides of the catalyst. In this test the XRD patterns of the alumina catalyst support show the presence of g-Al_2O_3 and traces of q-Al_2O_3. In order to calculate the average particle diameter of metal oxides, Scherrer's equation t ¼ 0:9l=ðB cos qÞ, is applied. The average particle diameter of NiO is 17.9 nm in Ni/Al_2O_3 catalyst and CuO is 17.4 nm in Cu/ ZnO/Al_2O_3 catalyst. XRD patterns of $NieCu/Al_2O_3$ proved the formation of Ni_XCu_{1-X} O and a shift in peaks compared to commercial catalyst are present. The average particle crystallite diameter of prepared catalyst is 19.3 nm. This can be related to more crystallites in the particles of Ni or Cu with respect to the commercial catalyst.

3.4 IR test

Fig. 4 shows the infrared spectra for the prepared and commercial catalysts. Applying infrared spectra for catalysts showed high and low wavenumber regions. At low wave-number regions, NieCu/Al_2O_3 catalyst showed three active peaks, of which two might result from pure Ni (1375 cm^{-1}) and Cu particles (1502 cm^{-1}), in addition a third peak for an alloy of NieCu particles (1643 cm^{-1}) as shown in Fig. 4. High wave-number region (3386 cm^{-1}) could be related to Ni surface spinel [45]. Band positions are affected by various variables such as temperature, surface concentrations, and the presence of other adsorbed species [45,46]. Therefore, the prepared catalyst showed shift in peaks compared to the commercial catalysts which is explained later in TPR test. At least three different oxide phases were detected in the spectra for the Ni commercial system: Al_2O_3, NiO and the so-called nickel surface spinel appeared in infrared test as reported by Ryczkowski [45]. The peaks were located at wavenumbers of 1028 cm^{-1}, 1444 cm^{-1} and 3386 cm^{-1} respectively. The commercial copper spectra displayed a band at 1515 cm^{-1} (CuO) and 3311 cm^{-1} (ZnO) which agree with the Edwards and Schrader study [46].

3.5 TPR test

Hydrogen uptakes (Fig. 5) for Cu/ZnO/Al_2O_3 catalyst showed one peak at 255 ^oC. The TPR trace for Ni/Al_2O_3 catalyst displayed two peaks at 670 ^oC and 776 ^oC, which were interpreted as weak and strong interactions between NiO and the Al_2O_3 support respectively [32,47,48].

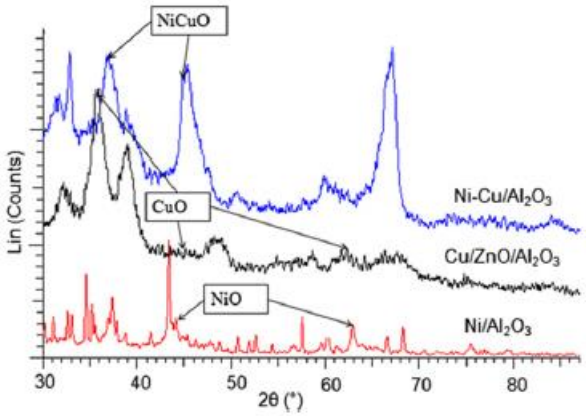

Fig. 3 – XRD diffraction patterns for commercial and prepared catalysts.

Three hydrogen uptake peaks were displayed on prepared NieCu/Al_2O_3 catalyst. The first peak at 180 ^oC is related to interactions between the CuO and Al_2O_3 support. The next broad peak at 390 ^oC is associated with NieCu alloy particles and the last peak at 620 ^oC might be due to NiO reduction. TPR data obtained from

commercial copper catalyst was totally agreed with TPR test carried out (250 ^{o}C) by Samuel and Hagelin [37]. Two reduction bands displayed by Ni catalyst are associated firstly with the reduction of nickel oxide interacting with alumina and secondly a high reduction band is attributed to the reduction of nickel aluminate phase [44]. TPR profiles of supported nickel catalysts are strongly affected by the nature of metal-support interaction [49]. NiO species supported on Al_2O_3 are reduced at around 500-700 ^{o}C and the reduction of nickel aluminate occurs at higher temperature above 800 ^{o}C because of the strong interaction between nickel species and alumina [50]. NieCu catalyst supported on Al_2O_3 prepared by De Rogatis et al [32] agrees with the TPR test reported in this work and showed three TPR peaks. In their study, the first reduction peak appeared at about 160 ^{o}C and was associated with the reduction of CuO. The second peak at 390 ^{o}C which was attributed to the reduction of Ni-based species promoted by the presence of metallic Cu as mentioned by Lee et al. [51]. The third peak at about 770 ^{o}C was related to strong interaction of Ni oxides species with the Al_2O_3. The difference in the position of reduction peaks reported in this work (Fig. 5) is related to the fact that reduction peaks strongly depend on the particle dimension and the interaction strength between metal particles and the support.

3.6. Activity test

H_2 selectivity (equation (7)), fuel conversion (equations (8) and (9)), CO_2 and CO selectivity (equations (10) and (11)) were investigated for both fuels and catalysts. These were calculated from the following equations:

$$H_2 \text{ selectivity} = \frac{[H_2]}{[H_2] + [CO_2] + [CO]} \cdot 100 \quad (7)$$

$$\text{Methanol conversion} = \frac{CH_3OH_{in} - CH_3OH_{out}}{CH_3OH_{in}} \cdot 100 \quad (8)$$

$$\text{Methane conversion} = \frac{CH_{4in} - CH_{4out}}{CH_{4in}} \cdot 100 \quad (9)$$

Table 3 – Physical characteristics of tested catalysts.

Characteristics	$Cu/ZnO/Al_2O_3$ (commercial)	Ni/Al_2O_3 (commercial)	$Ni–Cu/Al_2O_3$ (prepared)
Composition[a]	Cu = 50% ZnO = 25% Al_2O_3 = 25%	Ni = 40% Al_2O_3 = 60%	Ni = 5% Cu = 5% Al_2O_3 = 90%
Nitrogen BET area (m^2/g)	74	12	93
Pore volume (ml/g)	0.22	0.06	0.45
Active metal area (m^2/g)	1.32	8.62	11.38
Dispersion	0.21%	1.29%	1.74%
Crystallite size (Å)	119	187	193

a As provided from manufacturer data sheets or tested by XRF for prepared catalyst.

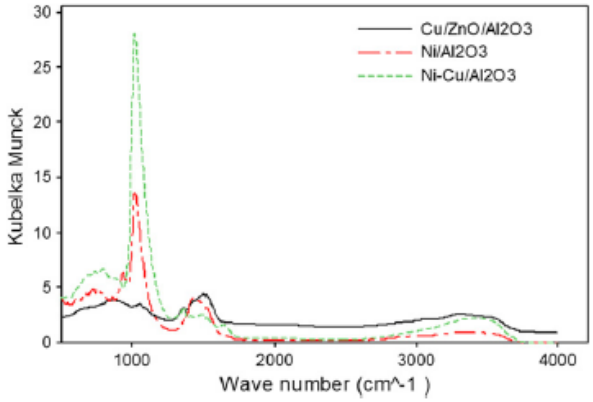

Fig. 4 – Infrared spectra for commercial and prepared catalysts.

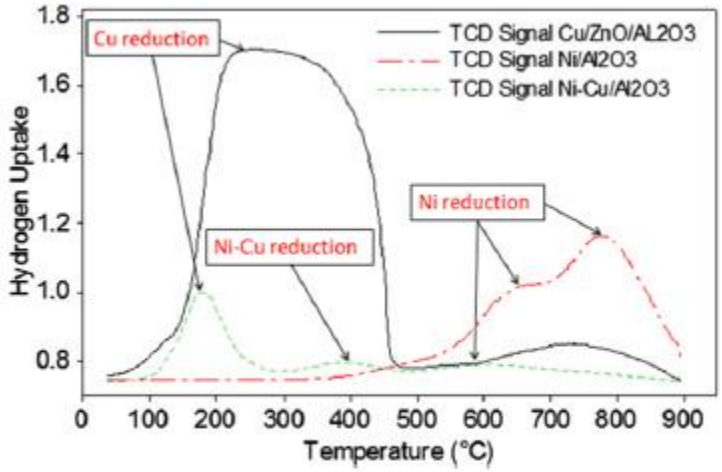

Fig. 5 – TPR of commercial and prepared catalysts.

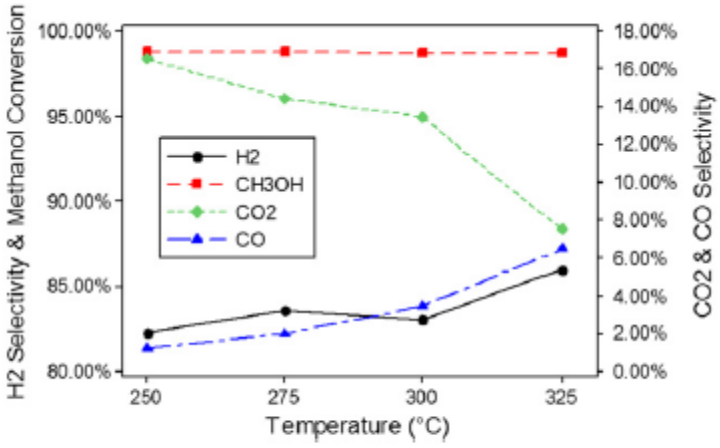

Fig. 6 – Methanol steam reforming over $Cu/ZnO/Al_2O_3$ catalyst.

$$CO_2 \text{ selectivity} = \frac{[CO_2]}{[CO_2] + [H_2] + [CO]} \cdot 100 \quad (10)$$

$$CO \text{ selectivity} = \frac{[CO]}{[CO] + [H_2] + [CO_2]} \cdot 100 \quad (11)$$

Fig. 6 shows methanol steam reforming over commercial $Cu/ZnO/Al_2O_3$ catalyst. Methanol conversion was 99% and hydrogen selectivity was 86% at 325 ^{o}C. With increasing temperature from 250 ^{o}C to 325 ^{o}C, the catalyst selectivity towards CO increased and CO_2 decreased. Investigating methanol steam reforming using prepared $NieCu/Al_2O_3$ as presented in Fig. 7 resulted in 99% methanol conversion and hydrogen selectivity was 89% at 275 ^{o}C. In contrast to commercial methanol steam reforming catalyst, $NieCu/Al_2O_3$ catalyst selectivity towards CO with increased temperature decreased and CO_2 selectivity increased as can be observed from the data shown in Table 4.

Methanol steam reforming could be assumed to be the sequence of methanol decomposition reaction (equation (3)) followed by water gas shift reaction (equation (4)) [18]. As a result, Peppley et al. [19] proposed two active sites on copper based catalyst. One site is responsible of steam reforming reaction and water gas shift reaction while the second site activates the decomposition reaction. The increase on CO selectivity over commercial $Cu/ZnO/Al_2O_3$ with increasing the temperature is related to high active reverse water gas shift reaction.

Table 4 – Gas feed composition for methanol steam reforming at various operating conditions.

Temperature (°C)	H_2 selectivity $Cu/ZnO/Al_2O_3$	H_2 selectivity $Ni-Cu/Al_2O_3$	CO_2 selectivity $Cu/ZnO/Al_2O_3$	CO_2 selectivity $Ni-Cu/Al_2O_3$	CO selectivity $Cu/ZnO/Al_2O_3$	CO selectivity $Ni-Cu/Al_2O_3$	Conversion $Cu/ZnO/Al_2O_3$	Conversion $Ni-Cu/Al_2O_3$
250	82.3%	85.5%	16.6%	9.2%	1.2%	5.3%	98.8%	98.3%
275	83.6%	89.1%	14.4%	9.9%	2.0%	1.0%	98.8%	98.4%
300	83.1%	86.2%	13.5%	12.9%	3.5%	0.8%	98.7%	98.7%
325	86.0%	87.4%	7.5%	11.9%	6.5%	0.7%	98.7%	98.8%

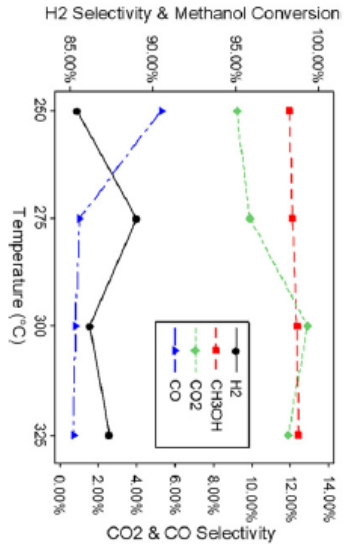

Fig. 7 – Methanol steam reforming over $Ni-Cu/Al_2O_3$ catalyst.

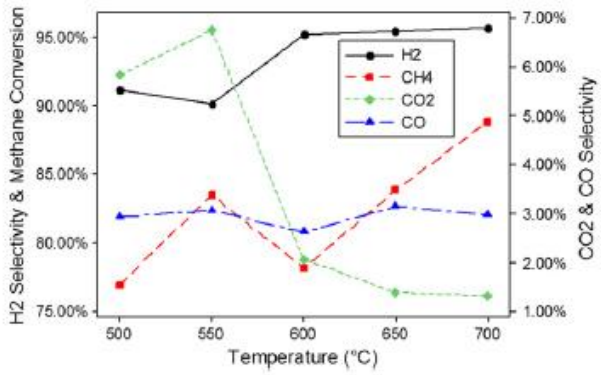

Fig. 8 – Methane steam reforming over Ni/Al_2O_3 catalyst.

However, this is not the case on prepared NieCu/ Al_2O_3 catalyst. The low selectivity towards CO suggests that water gas shift reaction is the dominant reaction at high temperature which can be related to fact that Cu doesn't easily dissociate CO [52] which leads to decrease on CO/CO_2 hydrogenation activity of Ni catalyst [33].

Methane steam reforming reaction over commercial Ni/ Al_2O_3 catalyst showed 89% methane fuel conversion and 96% for hydrogen selectivity at 700 ^{0}C (Fig. 8). The catalyst selectivity for CO with increasing temperature increased and CO_2 selectivity decreased as presented in Fig. 8. The same reaction (Fig. 9) was applied on prepared $NieCu/Al_2O_3$ catalyst and 89% of methane fuel conversion was achieved at 650 ^{0}C with 99% hydrogen selectivity at the same temperature. Increasing the temperature, the prepared $NieCu/Al_2O_3$ catalyst displayed a lower selectivity for CO and CO_2 in comparison with commercial Ni/Al_2O_3 catalyst as illustrated in Table 5.

Methane steam reforming is represented by three predominant reactions (equations (4)-(6)) [53]. Since methane steam reforming is very endothermic, the reaction temperature will significantly affect the equilibrium compositions of the product as well as the conversion [54]. Increasing the temperature (500-700 ^{0}C) both commercial Ni/Al_2O_3 and prepared $NieCu/Al_2O_3$ conversion.

Table 5 – Gas feed composition for methane steam reforming at various operating conditions.

Temperature (°C)	H_2 selectivity Ni/Al_2O_3	H_2 selectivity $Ni–Cu/Al_2O_3$	CO_2 selectivity Ni/Al_2O_3	CO_2 selectivity $Ni–Cu/Al_2O_3$	CO selectivity Ni/Al_2O_3	CO selectivity $Ni–Cu/Al_2O_3$	Conversion Ni/Al_2O_3	Conversion $Ni–Cu/Al_2O_3$
500	91.2%	99.1%	5.8%	0.7%	2.9%	0.3%	77.0%	86.3%
550	90.2%	98.1%	6.8%	1.1%	3.1%	0.8%	83.6%	82.7%
600	95.3%	98.8%	2.1%	0.8%	2.6%	0.4%	78.2%	86.2%
650	95.4%	99.0%	1.4%	0.6%	3.2%	0.3%	83.9%	89.2%
700	95.7%	98.8%	1.3%	0.8%	3.0%	0.4%	88.9%	88.7%

Fig. 9 – Methane steam reforming over $Ni–Cu/Al_2O_3$ catalyst.

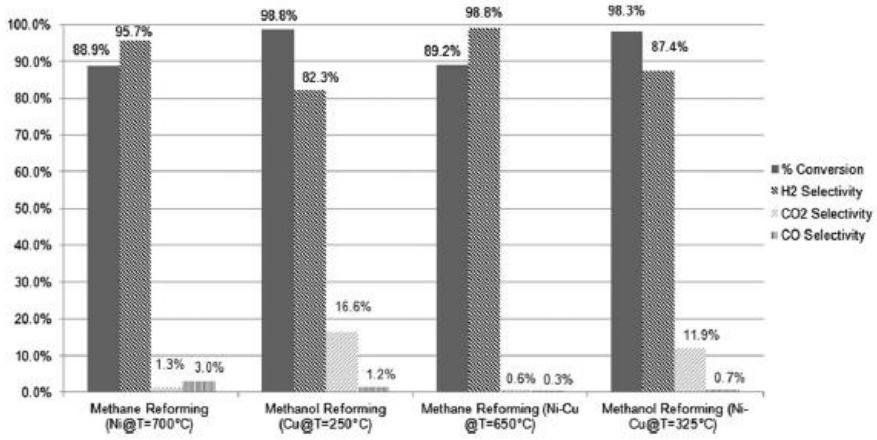

Fig. 10 – Optimal reforming results for both fuels and catalysts tested.

However, prepared NieCu/Al_2O_3 showed a low selectivity towards CO and CO_2 than commercial Ni/Al_2O_3 catalyst. This can be related to fact that NieCu alloy could be responsible for the blocking and decrease of the sites involved in the carbon growth [31] as explained in Boudouard reaction (equation (12)) [55]. Therefore, the Cu addition suppresses the carbon deposition and act as stabilizing agent in NieCu/Al_2O_3 atalyst [32,51].

$$2CO \rightarrow C + CO_2 \qquad (12)$$

Fig. 10 presents optimal steam reforming results in both fuels and all catalysts tested based on CO selectivity. Methanol reforming catalyst was less selective for CO than commercial methane reforming catalyst. The prepared catalyst was less selective for CO in comparison with both commercial Ni and Cu based catalysts. In addition, methane steam reforming can be carried out at lower temperature on NieCu catalyst (650 ^{o} C). However, reaction over commercial methane reforming catalyst is carried out at 700 ^{o} C. The low temperature of conversion is important for system material selection as well as requiring less external heating and insulation, all of which can lead to a smaller, more efficient integrated fuel cell reformer system [15]. As well as the low levels of CO formation on active catalyst will reduce the size of CO cleaning unit which can demonstrate compact fuel reformer for portable and onboard applications [56].

Thermo gravimetric analysis (TGA) was carried out for used catalysts at high and low temperature. The commercial Ni/Al_2O_3 catalyst resulted in high coke formation (28.3%) compared to prepared NieCu/Al_2O_3 (8.9%) and commercial Cu/ZnO/Al_2O_3 (3.5%) catalysts as shown in Fig. 11 and illustrated in Table 6. It is known that deactivation of Ni based catalysts can be due to carbon formation during reaction [57,58]. This was clearly suppressed by copper addition in NieCu/Al_2O_3 catalyst [51].

De Rogatis et al. [33] studied the catalytic performance of the bimetallic system of NieCu/Al_2O_3. They found that methanol conversion starts above 150 ^{0}C and the complete conversion is reached around 205 ^{0}C. CO_2 and CO product distributions follow opposite trends at temperatures below 300 ^{0}C, which strongly agrees with the results presented here. In the same study, no significant deactivation of catalyst activity and carbon formation was observed as proven by the TGA test reported here.

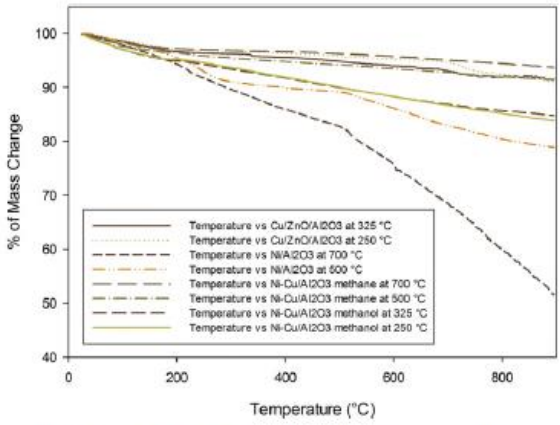

Fig. 11 – TGA of commercial and prepared catalysts.

Table 6 – Percentage of mass change of commercial and prepared catalysts at various operating conditions.

Catalyst	% of Mass change
Cu/ZnO/Al_2O_3 at 325 °C	3.2
Cu/ZnO/Al_2O_3 at 250 °C	3.5
Ni/Al_2O_3 at 700 °C	28.3
Ni/Al_2O_3 at 500 °C	16.4
Ni–Cu/Al_2O_3 methane at 700 °C	2.9
Ni–Cu/Al_2O_3 methane at 500 °C	3.7
Ni–Cu/Al_2O_3 methanol at 325 °C	8.3
Ni–Cu/Al_2O_3 methanol at 250 °C	8.9

Huang et al. [59] used a copper commercial catalyst as a reference in their study. The commercial catalyst showed 70% methanol conversion at a temperature of 300 ^{0}C. This can be related to the composition of catalyst and the low steam to methanol ratio applied. Matsumura and Ishibe [60] also used commercial copper catalyst as a reference. They reported 1.1% selectivity of CO and 59% of methanol conversion at a temperature of 300 ^{0}C and low steam to methanol ratio. Seo et al. [54] mentioned in their thermal energy analysis study the favourable operating conditions for steam reforming of methane. They achieved 99% methane conversion at a steam to carbon ratio of 1.9 and reactor temperature of 800 ^{0} C. The commercial nickel catalyst here showed a similar trend for fuel conversion and gaseous selectivity and strongly confirmed the gas product composition published by Heinzel et al. [23]. Both methane tested catalysts showed better hydrogen selectivity and methane

conversion trends at temperatures above 600 ^{0} C with lower selectivity for CO than previous thermodynamic studies [21,54,61]. To the best of the author's knowledge, it was difficult to find a literature study that had tested NieCu/Al_2O_3 on methane steam reforming [62]. However, the study carried by Huang and Jhao [63] proved that NieCu interaction enhances the activity of steam reforming of methane and decreases the CO production rate as shown in the activity test reported here.

4. Conclusions

The results of characterization showed that the prepared NieCu/Al_2O_3 catalyst is reduced at 390 ^{0} C. Various types of metal interactions with the support are present in the TPR test. In NieCu/Al_2O_3 catalyst, Cu particles increase the active particle size of Ni (19.3 nm) in NieCu/Al_2O_3 catalyst with respect to the commercial Ni/Al_2O_3 (17.9 nm). On the other hand, Ni improves Cu dispersion in the same catalyst (1.74%) in comparison with commercial Cu/ZnO/Al_2O_3 (0.21%). NieCu/ Al_2O_3 showed a high BET surface area compared to the commercial catalysts. XRD patterns of NieCu/Al_2O_3 proved the formation of $Ni_xCu_{1-x}O$ and there is a shift of peaks compared to commercial catalyst. IR test at low frequency showed three peaks in NieCu/Al_2O_3 which are related to pure Ni and Cu metal plus an alloy of NieCu particles.

A comprehensive comparison between two fuels is established in term of reaction conditions, fuel conversion, H_2 selectivity, CO_2 selectivity and CO selectivity. The prepared catalyst showed lower selectivity for CO in both fuels and NieCu catalyst was more selective to H_2 compared to commercial catalysts. Methanol steam reforming over commercial Cu/ZnO/Al_2O_3 catalyst showed 99% fuel conversion and hydrogen selectivity was 86% at 325 ^{0} C. NieCu/Al_2O_3 resulted in 99% methanol conversion and hydrogen selectivity was 89% at 275 ^{0} C. Investigating methane steam reforming reaction over commercial Ni/Al_2O_3 catalyst showed 89% methane fuel conversion and 96% for hydrogen selectivity at 700 ^{0}C. The prepared NieCu/Al_2O_3 catalyst achieved 89% of methane fuel conversion and 99% hydrogen selectivity at 650 ^{0} C. Methanol steam reforming is carried out at a much lower temperature (275-325 ^{0}C) than needed in methane reforming. However, methane steam reforming can be carried out at a relatively low temperature on NieCu catalyst (600-650 ^{0} C) and at higher temperature in commercial methane reforming catalyst (700-800 ^{0} C). TGA test showed that commercial Ni/Al_2O_3 catalyst resulted in high coke formation (28.3% loss in mass) compared to prepared NieCu/ Al_2O_3 (8.9%) and commercial Cu/ZnO/Al_2O_3 catalysts (3.5%). This can be related to fact that NieCu alloy is responsible for the blocking and decrease of the sites involved in the carbon growth during methane steam reforming reaction.

Therefore, the Cu addition suppresses the carbon deposition and acts as stabilizing agent in NieCu/Al_2O_3 during steam reforming reaction.

Acknowledgements
Centre for Applied Energy Research (CAER-int, Jordan) is acknowledged for the financial support.

References

[1] Ball M, Wietschel M. The future of hydrogen e opportunities and challenges. International Journal of Hydrogen Energy 2009;34:615e27.

[2] Mueller-Langer F, Tzimas E, Kaltschmitt M, Peteves S. Techno-economic assessment of hydrogen production processes for the hydrogen economy for the short and medium term. International Journal of Hydrogen Energy 2007;32:3797e810.

[3] Budzianowski WM. Value-added carbon management technologies for low CO_2 intensive carbon-based energy vectors. Energy 2012;41:280e97.

[4] Larminie J, Dicks A. Fuel cell systems explained. 2nd ed. Wiley; 2003.

[5] Xuan J, Leung MKH, Leung DYC, Ni M. A review of biomass-derived fuel processors for fuel cell systems. Renewable and Sustainable Energy Reviews 2009;13:1301e13.

[6] Kolb G. Fuel processing for fuel cells. Weinheim: Wiley-VCH; 2008.

[7] Ahmed S, Kumar R, Krumpelt M. Fuel processing for fuel cell power systems. Fuel Cells Bulletin 1999;2:4e7.

[8] Cipitì F, Pino L, Vita A, Laganà M, Recupero V. Performance of a 5 kWe fuel processor for polymer electrolyte fuel cells. International Journal of Hydrogen Energy 2008;33:3197e203. [9] Faur Ghenciu A. Review of fuel processing catalysts for hydrogen production in PEM fuel cell systems. Current Opinion in Solid State and Materials Science 2002;6:389e99.

[10] Budzianowski WM. An oxy-fuel mass-recirculating process for H_2 production with CO_2 capture by autothermal catalytic oxyforming of methane. International Journal of Hydrogen Energy 2010;35:7454e69.

[11] Clarke SH, Dicks AL, Pointon K, Smith TA, Swann A. Catalytic aspects of the steam reforming of hydrocarbons in internal reforming fuel cells. Catalysis Today 1997;38:411e23.

[12] Qi A, Peppley B, Karan K. Integrated fuel processors for fuel cell application: a review. Fuel Processing Technology 2007; 88:3e22.

[13] Brown LF. A comparative study of fuels for on-board hydrogen production for fuel-cell-powered automobiles. International Journal of Hydrogen Energy 2001;26:381e97.

[14] Lindströ m B, Pettersson LJ. Development of a methanol fuelled reformer for fuel cell applications. Journal of Power Sources 2003;118:71e8.

[15] Palo DR, Dagle RA, Holladay JD. Methanol steam reforming for hydrogen production. Chemical Reviews 2007;107:3992e4021. [16] McNicol BD, Rand DAJ, Williams KR. Fuel cells for road transportation purposes d yes or no? Journal of Power Sources 2001;100:47e59.

[17] Joensen F, Rostrup-Nielsen JR. Conversion of hydrocarbons and alcohols for fuel cells. Journal of Power Sources 2002;105: 195e201.

[18] Peppley BA, Amphlett JC, Kearns LM, Mann RF. Methanolesteam reforming on $Cu/ZnO/Al_2O_3$. Part 1: the reaction network. Applied Catalysis A: General 1999;179:21e9.

[19] Peppley BA, Amphlett JC, Kearns LM, Mann RF. Methanolesteam reforming on $Cu/ZnO/Al_2O_3$ catalysts. Part 2. A comprehensive kinetic model. Applied Catalysis A: General 1999;179:31e49.
[20] Lwin Y, Daud WRW, Mohamad AB, Yaakob Z. Hydrogen production from steamemethanol reforming: thermodynamic analysis. International Journal of Hydrogen Energy 2000;25:47e53.
[21] Á vila-Neto CN, Dantas SC, Silva FA, Franco TV, Romanielo LL,
Hori CE, et al. Hydrogen production from methane reforming: thermodynamic assessment and autothermal reactor design. Journal of Natural Gas Science and Engineering 2009;1:205e15.
[22] Matsumura Y, Nakamori T. Steam reforming of methane over nickel catalysts at low reaction temperature. Applied Catalysis A: General 2004;258:107e14.
[23] Heinzel A, Vogel B, Hü bner P. Reforming of natural gasdhydrogen generation for small scale stationary fuel cell systems. Journal of Power Sources 2002;105:202e7.
[24] Richardson JT. Principles of catalyst development. New York: Plenum Press; 1989.
[25] De Rogatis L, Montini T, Lorenzut B, Fornasiero P. $NiCu/Al_2O_3$ based catalysts for hydrogen production. Energy & Environmental Science 2008;1:501e9.
[26] Carrero A, Calles JA, Vizca´ıno AJ. Hydrogen production by ethanol steam reforming over CueNi/SBA-15 supported catalysts prepared by direct synthesis and impregnation. Applied Catalysis A: General 2007;327:82e94.
[27] Vizcaí no AJ, Carrero A, Calles JA. Hydrogen production by ethanol steam reforming over CueNi supported catalysts. International Journal of Hydrogen Energy 2007;32:1450e61.
[28] Mariñ o F, Boveri M, Baronetti G, Laborde M. Hydrogen production from steam reforming of bioethanol using Cu/Ni/ K/g-Al_2O_3 catalysts. Effect of Ni. International Journal of Hydrogen Energy 2001;26:665e8.
[29] Echegoyen Y, Suelves I, Lá zaro MJ, Moliner R, Palacios JM. Hydrogen production by thermocatalytic decomposition of methane over NieAl and NieCueAl catalysts: effect of calcination temperature. Journal of Power Sources 2007;169: 150e7.
[30] Chen J, Li Y, Li Z, Zhang X. Production of CO_x-free hydrogen and nanocarbon by direct decomposition of undiluted methane on NieCuealumina catalysts. Applied Catalysis A: General 2004;269:179e86.
[31] Reshetenko TV, Avdeeva LB, Ismagilov ZR, Chuvilin AL, Ushakov VA. Carbon capacious $NieCueAl_2O_3$ catalysts for high-temperature methane decomposition. Applied Catalysis A: General 2003;247:51e63.
[32] De Rogatis L, Montini T, Cognigni A, Olivi L, Fornasiero P. Methane partial oxidation on NiCu-based catalysts. Catalysis Today 2009;145:176e85.
[33] De Rogatis L, Montini T, Lorenzut B, Fornasiero P. Ni_xCu_y/ Al_2O_3 based catalysts for hydrogen production. Energy & Environmental Science 2008;1:501e9.

[34] Brunauer S, Emmett PH, Teller E. Adsorption of gases in multimolecular layers. Bureau of Chemistry and Soils and George Washington University; 1938.
[35] Oliveira ELG, Grande CA, Rodrigues AE. Steam methane reforming in a Ni/Al_2O_3 catalyst: kinetics and diffusional limitations in extrudates. The Canadian Journal of Chemical Engineering 2009;87:945e56.
[36] Hou K, Hughes R. The kinetics of methane steam reforming over a Ni/a-Al_2O catalyst. Chemical Engineering Journal 2001; 82:311e28.
[37] Jones SD, Hagelin-Weaver HE. Steam reforming of methanol over CeO_2- and ZrO_2-promoted CueZnO catalysts supported on nanoparticle Al_2O_3. Applied Catalysis B: Environmental 2009;90:195e204.
[38] Gine´ s MJL, Amadeo N, Laborde M, Apesteguı´a CR. Activity and structure-sensitivity of the wateregas shift reaction over CuZnAl mixed oxide catalysts. Applied Catalysis A: General 1995;131:283e96.
[39] Yao C-Z, Wang L-C, Liu Y-M, Wu G-S, Cao Y, Dai W-L, et al. Effect of preparation method on the hydrogen production from methanol steam reforming over binary Cu/ZrO_2 catalysts. Applied Catalysis A: General 2006;297:151e8.
[40] Shishido T, Yamamoto Y, Morioka H, Takaki K, Takehira K. Active Cu/ZnO and $Cu/ZnO/Al_2O_3$ catalysts prepared by homogeneous precipitation method in steam reforming of methanol. Applied Catalysis A: General 2004;263:249e53.
[41] Shishido T, Yamamoto Y, Morioka H, Takehira K. Production of hydrogen from methanol over Cu/ZnO and $Cu/ZnO/Al_2O_3$ catalysts prepared by homogeneous precipitation: steam reforming and oxidative steam reforming. Journal of Molecular Catalysis A: Chemical 2007;268:185e94.
[42] Á guila G, Jime´ nez J, Guerrero S, Gracia F, Chornik B, Quinteros S, et al. A novel method for preparing high surface area copper zirconia catalysts: influence of the preparation variables. Applied Catalysis A: General 2009;360:98e105.
[43] Oliveira ELG, Grande CA, Rodrigues AE. Methane steam reforming in large pore catalyst. Chemical Engineering Science 2010;65:1539e50.
[44] Seo JG, Youn MH, Jung JC, Song IK. Effect of preparation method of mesoporous $NieAl_2O_3$ catalysts on their catalytic activity for hydrogen production by steam reforming of liquefied natural gas (LNG). International Journal of Hydrogen Energy 2009;34:5409e16.
[45] Ryczkowski J. IR spectroscopy in catalysis. Catalysis Today 2001;68:263e381.
[46] Edwards JF, Schrader GL. Infrared spectroscopy of copper/ zinc oxide catalysts for the wateregas shift reaction and methanol synthesis. The Journal of Physical Chemistry 1984; 88:5620e4.
[47] Roh H-S, Jun K-W, Dong W-S, Chang J-S, Park S-E, Joe Y-I. Highly active and stable $Ni/CeeZrO_2$ catalyst for H_2 production from methane. Journal of Molecular Catalysis A: Chemical 2002;181:137e42.
[48] Ye J, Li Z, Duan H, Liu Y. Lanthanum modified Ni/g-Al_2O_3 catalysts for partial oxidation of methane. Journal of Rare Earths 2006;24:302e8.
[49] Seo JG, Youn MH, Park S, Song IK. Effect of calcination temperature of mesoporous alumina xerogel (AX) supports on hydrogen production by steam

reforming of liquefied natural gas (LNG) over Ni/AX catalysts. International Journal of Hydrogen Energy 2008;33:7427e34.
[50] Youn MH, Seo JG, Kim P, Song IK. Role and effect of molybdenum on the performance of NieMo/g-Al_2O_3 catalysts in the hydrogen production by auto-thermal reforming of ethanol. Journal of Molecular Catalysis A: Chemical 2007;261:276e81.
[51] Lee J-H, Lee E-G, Joo O-S, Jung K-D. Stabilization of Ni/Al_2O_3 catalyst by Cu addition for CO_2 reforming of methane. Applied Catalysis A: General 2004;269:1e6.
[52] Ponec V. Selectivity in the syngas reactions: the role of supports and promoters in the activation of Co and in the stabilization of intermediates. In: Guczi L, editor. Studies in surface science and catalysis. Elsevier; 1991. p. 117e57 [chapter 4].
[53] Xu J, Froment GF. Methane steam reforming, methanation and wateregas shift: I. Intrinsic kinetics. AIChE Journal 1989; 35:88e96.
[54] Seo YS, Shirley A, Kolaczkowski ST. Evaluation of thermodynamically favourable operating conditions for production of hydrogen in three different reforming technologies. Journal of Power Sources 2002;108:213e25.
[55] Freni S, Calogero G, Cavallaro S. Hydrogen production from methane through catalytic partial oxidation reactions. Journal of Power Sources 2000;87:28e38.
[56] Arzamendi G, Dié guez PM, Montes M, Centeno MA, Odriozola JA, Gandí a LM. Integration of methanol steam reforming and combustion in a microchannel reactor for H_2 production: a CFD simulation study. Catalysis Today 2009; 143:25e31.
[57] Miao Q, Xiong G, Sheng S, Cui W, Xu L, Guo X. Partial oxidation of methane to syngas over nickel-based catalysts modified by alkali metal oxide and rare earth metal oxide. Applied Catalysis A: General 1997;154:17e27.
[58] Sperle T, Chen D, Lødeng R, Holmen A. Pre-reforming of natural gas on a Ni catalyst: criteria for carbon free operation. Applied Catalysis A: General 2005;282:195e204.
[59] Huang G, Liaw B-J, Jhang C-J, Chen Y-Z. Steam reforming of methanol over CuO/ZnO/CeO_2/ZrO_2/Al_2O_3 catalysts. Applied Catalysis A: General 2009;358:7e12.
[60] Matsumura Y, Ishibe H. Suppression of CO by-production in steam reforming of methanol by addition of zinc oxide to silica-supported copper catalyst. Journal of Catalysis 2009;268:282e9.
[61] Balasubramanian B, Lopez Ortiz A, Kaytakoglu S, Harrison DP. Hydrogen from methane in a single-step process. Chemical Engineering Science 1999;54:3543e52.
[62] Khzouz M, Wood J, Kendall K, Bujalski W. Characterization of NieCu-based catalysts for multi-fuel steam reformer. International Journal of Low-Carbon Technologies 2011. [63] Huang T-J, Jhao S-Y. NieCu/samaria-doped ceria catalysts for steam reforming of methane in the presence of carbon dioxide. Applied Catalysis A: General 2006;302:325e32.